研 究 速 報

Unsteady Flow Induced by Annular Cascade

入り口案内翼後流に発生する不安定流れ

Keishi SUMIYOSHI*, Nobuyuki TAKAMA*, Katsuhiko NISHIMURA* and Haruo YOSHIKI*

住 吉 圭 司・高 間 信 行・西 村 勝 彦・吉 識 晴 夫

1. Introduction

Research and development of an automotive ceramic gas turbine have been carried out in order to protect the global environment and to use many kinds of fuels. A small, efficient and reliable high speed centrifugal compressor is used for the automotive gas turbine and variable inlet guide vanes (VIGV) should be set at the inlet of the compressor to achieve high efficiency. Especially in lower flow rate, the VIGV angle measured from the radial direction is set much large and so the flow at the inlet of rotor has high rotational velocity. Under that flow condition, an unsteady flow with some superior components of frequency appears and the efficiency of the compressor decreases (Ref. 1). In this study, we certify the appearance of unsteady flow with unusual sound in the wake of annular cascade which corresponds to VIGV. Therefore, we measure the state of flow by a hot wire anemometer, semiconductor pressure transducers and a three-hole pitot tube. After recording those data to a personal computer, we make a data processing and visualization so that we may understand the phenomenon easily.

2. Apparatus

A schematic diagram of the experimental apparatus is shown in Fig. 1. At the inlet of the settling chamber of the suction-type wind tunnel, we connect a swirl generator to a straight pipe. Inflow air flows from atmosphere in the radial direction and then it is given peripheral velocity by the swirl generator with twenty-four guide vanes. After it is turned to the axial direction, it flows into the settling chamber through the straight pipe. In Fig. 1, St. 1 is the section where we measure the radial distributions of velocity, flow angle and pressure by the three-hole pitot tube. We can estimate the flow rate by the velocity distributions.

The swirl generator is shown in Fig. 2. It consists of a shroud side casing, a hub side casing, a lid and guide vanes. On the shroud side casing, there are twenty-four holes to set the guide vanes and short lines drawn for setting angle α of VIGV, which is measured from the radial direction. The guide vane is designed on NACA747, A-015 and is cut out at 90% of its chord length. The final sizes of vane are 70mm

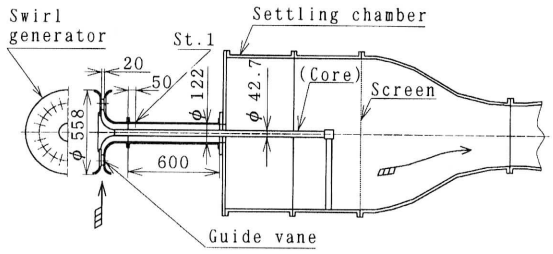

Fig. 1 Schematic diagram of experimental apparatus

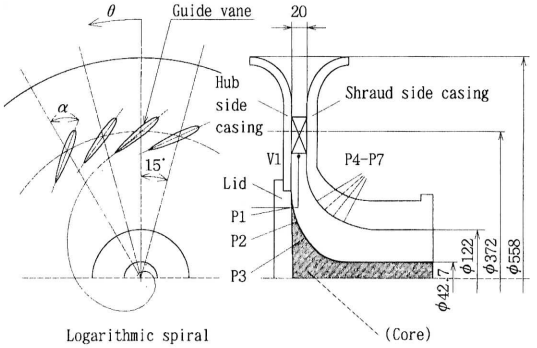

Fig. 2 Swirl generator

*Dept. of Mechanical Engineering and Naval Architecture, Institute of Industrial Science, University of Tokyo

in chord length, 11.25mm in maximum thickness and 20mm in height. The rotating axis of guide vane is located at 40% of its chord length. The hub side casing supports the lid, which is 220mm in diameter. In Fig. 2, V1 is the position where the hot wire anemometer is set at 160mm in radius corresponding to 10% chord length after the trailing edge. We can set circumferential angle θ arbitrarily by rotating the lid.

In this study, the lid with core or without core is used. The former has a core of 42.7mm in diameter, and so the straight pipe has an annular passage. In Fig.2, P1 to P3 indicate the measuring holes (0.5mm in diameter) of pressure on the lid wall (only in the case with core). They are arranged in radial direction from 90mm in radius at interval of about 20mm. By rotating the lid, we can set their circumferential position arbitrarily, too. P4 to P7 denote the measuring holes (0.5mm in diameter) of pressure on the shroud side casing wall. They are arranged in radial direction from 100mm in radius at interval of about 15mm. We set the semiconductor pressure transducers at the positions and measure unsteady pressure fluctuations by them.

3. Experimental Methods

To get the circumferential distributions of static pressure, we measure pressures at P1 to P3 every one degree of θ in the case with core only. And we measure pressures at P4 to P7, positions of which cannot be changed circumferentially. After transforming the pressure into an electric signal, we record it on a personal computer through A/D board, sampling frequency of which is 2.5kHz, and calculate its power-spectrum by FFT.

We measure circumferential distributions of velocity with the hot wire anemometer by rotating the lid by one degree. We treated the data in the same way as those of pressure.

On each experiment, we set the static pressure in the settling chamber approximately at -800, -600 and -400 Pa, and set the VIGV angle α at 30, 50 and 60 degrees, respectively.

4. Experimental Results

Figure 3 shows radial distributions of velocity at St. 1 in the cases with and without core. In the figure, u means axial flow velocity, w means circumferential flow velocity and r/R_0 means non-dimensional radial position. The cases of dotted lines (α=30°) are dominated by the free vortex flow region and solid lines (α=50°, 60°) are by the forced vortex flow region. From these data, the flow rate and the average axial velocity, Um, are calculated.

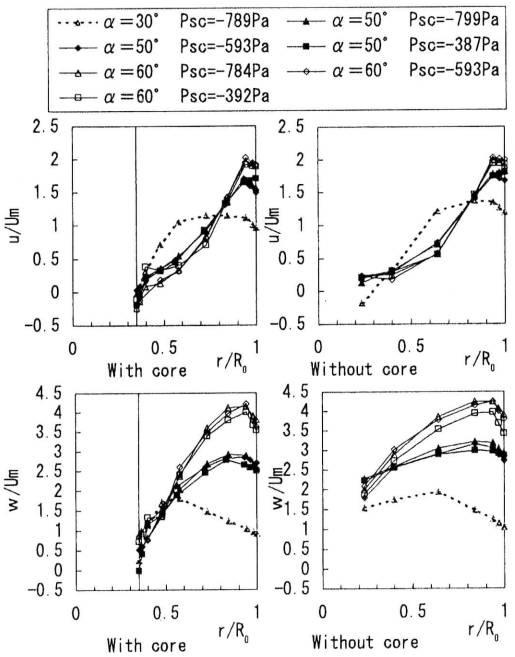

Fig. 3 Radial distributions of velocity at St. 1

Fig. 4 and Fig. 5 show the pressure waves on wall against time and their power-spectra against frequency. In the figures, Reynolds number is defined by UwC/ν, where Uw is the average flow velocity at inlet guide vanes, C is the cord length of guide vane and ν is the fluid viscosity.

From Fig. 4(a) (α=30°), we can image that the static pressure becomes lower and the flow velocity becomes higher as flowing downstream. And we cannot recognize any unsteady flow and hear any unusual sound. But in Fig.4 (b) (α=50°), we can observe the unusual sound and unsteady flow, the fundamental frequency of which is about 51Hz. And the pressure wave forms at P1 to P3 are different from those at P4 to P7, and especially the pressure fluctuation at P3 is large. The time-averaged pressure at P3 is smaller than that of P7 because of centrifugal force by swirl. As to the peaks of the power-spectra, the fundamental frequency dominates on P1 to P3, but the second and the third harmonies become higher on P4 to P7 as flowing downstream.

Figure 5 shows the pressure waves on wall against time and their power-spectra against frequency in the case without core. The figure indicates qualitatively similar to

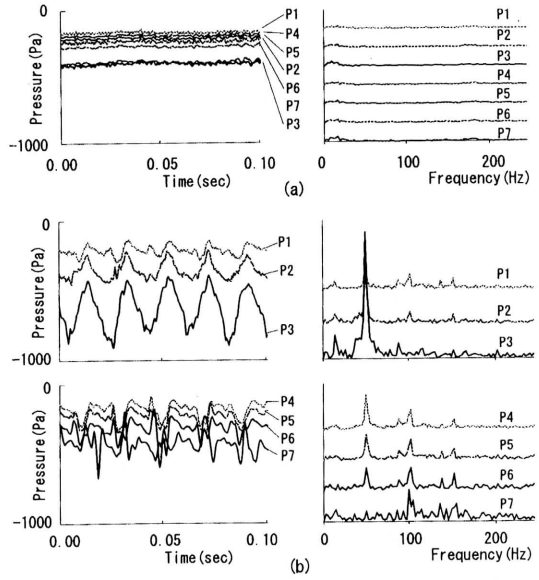

Fig. 4 Static pressure waves at P1 to P7 against time and their power-spectra against frequency in the case with core
(a) α =30°, Psc=-804Pa, Re=6.7×10^4
(b) α =50°, Psc=-784Pa, Re=4.8×10^4

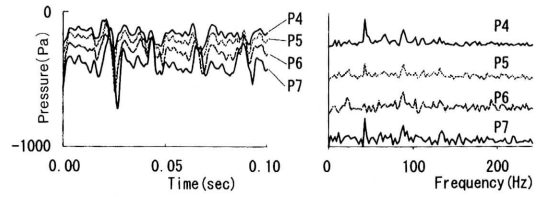

Fig. 5 Static pressure waves at P4 to P7 against time and their power-spectra against frequency in the case without core
α =50°, Psc=-799Pa, Re=4.8×10^4

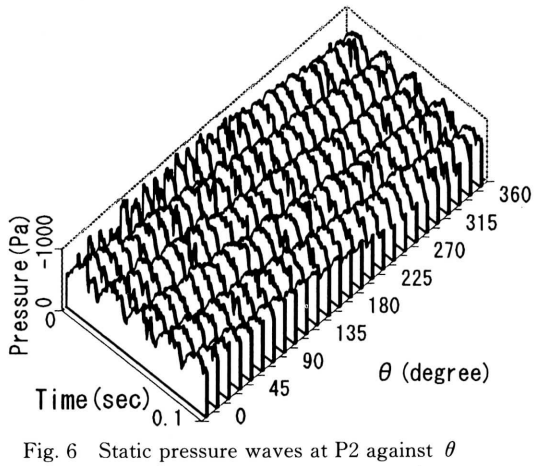

Fig. 6 Static pressure waves at P2 against θ
α =50°, Psc=-784Pa, Re=4.8×10^4, with core

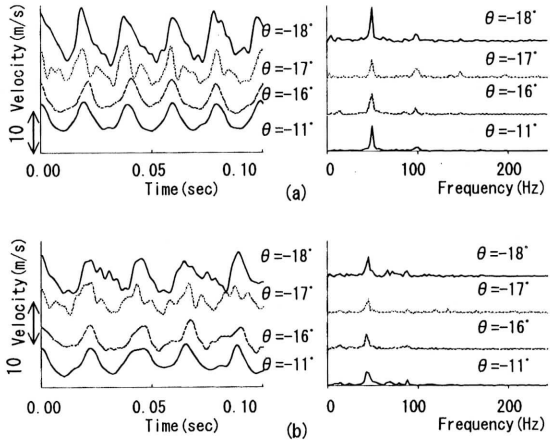

Fig. 7 Flow velocity waves at V1 against time and their power-spectra against frequency in the cases with and without core
(a) α =50°, Psc=-804Pa, Re=4.9×10^4, with core
(b) α =50°, Psc=-799Pa, Re=4.8×10^4, without core

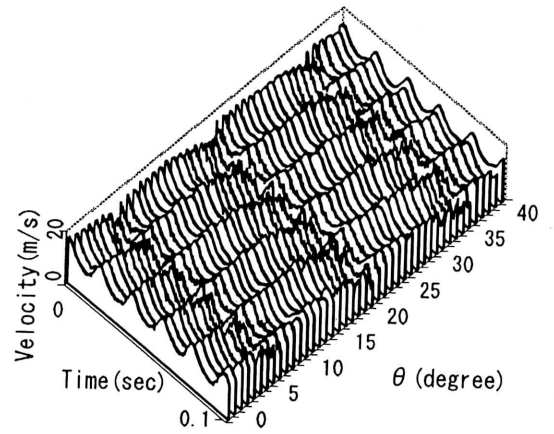

Fig. 8 Flow velocity waves at V1 against θ
α =50°, Psc=-784Pa, Re=4.8×10^4, with core

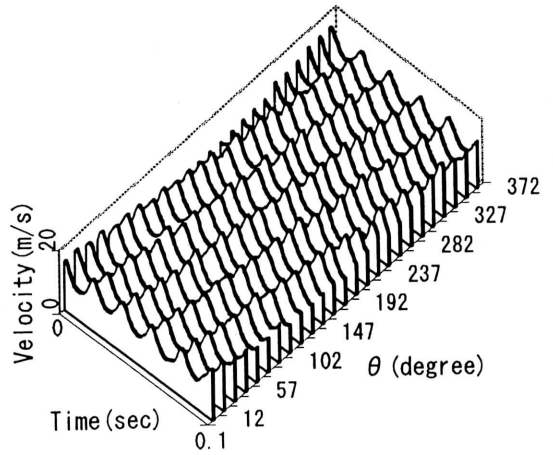

Fig. 9 Flow velocity waves at V1 against θ
α =50°, Psc=-784Pa, Re=4.8×10^4, with core

Fig.4 (b). The fundamental frequency of this case is about 46Hz.

Figure 6 shows the pressure waves measured at P2 against θ. It is supposed that if θ shifts 360°, the phase of pressure wave will shifts 360°, too. And if θ increases, the phase of pressure wave will be late.

Figure 7 shows the flow velocity waves at V1 against time and their power-spectra against frequency. In the figure, we use a 300Hz low-pass filter to make the wave form clear. At some typical points (θ=-18°, -17°, -16°, -11°), we compare wave forms with core and without core. The measurement point of θ=-17° corresponds to the wake of VIGV, θ=-16° to pressure side, θ=-18° to suction side and θ=-11° to the free stream of flow passage. Fig. 7(a) agrees qualitatively with Fig. 7(b). The fundamental frequency of the former is about 51Hz and that of the latter is about 46Hz. And the peaks of the power-spectra are same as those of pressure waves.

Figure 8 shows the flow velocity waves at V1 against θ. In the figure, θ is changed by one degree. From the figure, it makes clear that the effect of wake appears every fifteen degrees of θ, corresponded to a pitch of VIGV.

Figure 9 shows the flow velocity waves at V1 against θ. From this figure, we can see that the phase of velocity wave shifts 360° along θ. And if θ increases, the phase of velocity wave will be late, as is the pressure wave.

5. Discussion

Figure 10 shows Strouhal numbers against non-dimensional flow rate Q/Q_0, where Q is the flow rate and Q_0 is the flow rate at α=50° with core. Strouhal number is defined by fC/Uw, where f is the fundamental frequency of pressure wave. From this figure, it is supposed that Strouhal number is almost constant under each experimental condition.

Figure 11 shows the fundamental frequency of pressure wave against Reynolds number. It is considered that the frequency is proportional to Reynolds number under each experimental condition.

From Fig. 6 and Fig. 9, it is known that if θ increases, the phases of velocity and pressure waves will be late. But their directions are opposite to the phase shift of rotating stall in annular cascades. So we conclude this phenomenon is different from the usual rotating stall in annular cascades.

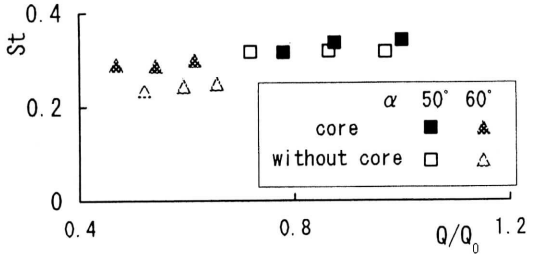

Fig. 10 Strouhal numbers against non-dimensional flow rate

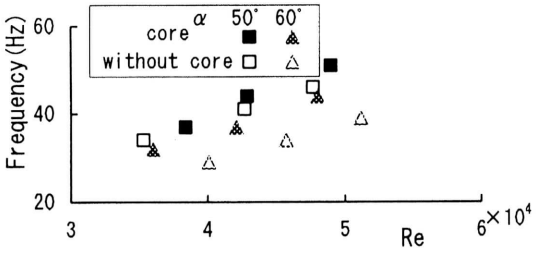

Fig. 11 Fundamental frequencies of pressure waves against Reynolds number

From Fig. 3, the flow pattern in straight pipe of α=30° without unusual sound much differs from that of α=50° with unusual sound. So it is imagined that the strong swirling flow makes unsteady flow somewhere behind the cascade.

6. Conclusion

As a result of experiments, the followings are found.

1. Unsteady flow with unusual sound is appeared behind the annular cascade under condition of $\alpha \geqq 50°$.
2. The frequency of unsteady flow is proportional to Reynolds number.
3. Unsteady flow is appeared in both cases with and without core.
4. Strouhal number is almost constant under each experimental condition.
5. Unsteady flow appeared in this experiment is different from the usual rotating stall.

(Manuscript received, June 9, 1995)

Reference

1) H. Uchida, A. Bessho, M. Shirai, H. Katagiri, Y. Yagi and T. Takamura , Journal of GTSJ, 21–84 (1994), 83–89